Radiation Protection Dosimetry Advance Access published November 18, 2015

Radiation Protection Dosimetry (2015), pp. 1–7 doi:10.1093/rpd/ncv473

AN EVALUATION OF THE BASIC CHARACTERISTICS OF A PLASTIC SCINTILLATING FIBRE DETECTOR IN CT RADIATION FIELDS

Kento Terasaki, Toshioh Fujibuchi*, Takatoshi Toyoda, Yutaka Yoshida, Tsutomu Akasaka, Akihiro Nohtomi and Junji Morishita
Department of Health Sciences, Graduate School of Medical Sciences, Kyushu University, 3-1-1 Maidashi, Higashi-ku, Fukuoka 812-8582, Japan

*Corresponding author: fujibuch@hs.med.kyushu-u.ac.jp

Received 28 July 2015; revised 13 September 2015; accepted 9 October 2015

The ionisation chamber for computed tomography (CT) is an instrument that is most commonly used to measure the computed tomography dose index. However, it has been reported that the 10 cm effective detection length of the ionisation chamber is insufficient due to the extent of the dose distribution outside the chamber. The purpose of this study was to estimate the basic characteristics of a plastic scintillating fibre (PSF) detector with a long detection length of 50 cm in CT radiation fields. The authors investigated position dependence using diagnostic X-ray equipment and dependencies for energy, dose rate and slice thickness using an X-ray CT system. The PSF detector outputs piled up at a count rate of 10 000 counts ms^{-1} in dose rate dependence study. With calibration, this detector may be useful as a CT dosemeter with a long detection length except for the measurement at high dose rate.

INTRODUCTION

The number of X-ray computed tomography (CT) systems in Japan reached 101.3 per 1 million people in 2011[1]. Due to the increased performance of X-ray CT examinations, patients and operators are exposed to increasing radiation doses. Recently, this has become a matter of concern. Thus, the accurate determination of doses of patients and operators as well as the management of X-ray CT systems is viewed as important. The computed tomography dose index (CTDI)[2–6] is the major radiation dosage index. $CTDI_{100}$ is commonly measured using an ionisation chamber of 10 cm in length and a standardised phantom of 16 or 32 cm in diameter. $CTDI_{100}$ is defined as follows:

$$CTDI_{100} = \frac{1}{nT}\int_{-50\,mm}^{50\,mm} K(z)dz,$$

where $K(z)$ is the air kerma in the phantom as a function of position on the z axis. In the case of $CTDI_{100}$, the integration limits are ± 50 mm, which corresponds to the 100 mm length of the ionisation chamber. n is the number of tomographic sections imaged in a single axial scan. T is the nominal width of the tomographic section along the z axis. $CTDI_w$ is intended as an average value, calculated from the $CTDI_{100}$ centre and peripheral measurements. Therefore, $CTDI_w$ is defined as follows:

$$CTDI_w = \frac{1}{3}CTDI_{100,\,center} + \frac{2}{3}CTDI_{100,\,peripheral}.$$

$CTDI_{vol}$ is a useful dose metric because it takes into account the important parameter of pitch. Pitch is defined as the ratio of the table travel per rotation. And its value is displayed on the console of CT scanners. $CTDI_{vol}$ is defined as follows:

$$CTDI_{vol} = \frac{1}{Pitch}CTDI_w.$$

A dose profile, with a bell curve distribution, is formed in the CTDI phantom with a single X-ray CT scan (Figure 1). A rectangular profile, which is limited to slice thickness, is obtained without scattering. X-ray absorption and scattering yields a bell curve-shaped dose profile, as shown in Figure 1. It is reported that the ionisation chambers in general use for the measurement of CTDI cannot cover the extended dose distribution especially in multidetector row CT. Thus, the measurements using an ionisation chamber may lead to the underestimation of radiation doses[7, 8]. To solve this issue, the authors proposed the use of a plastic scintillating fibre (PSF), which has the ability to process various detection lengths. As an example of other applications of the PSF, this has been developed for the dosimetry of high-energy beam in radiotherapy[9]. In this paper, in order to verify the usefulness of the PSF detector in CT radiation fields, the authors evaluated the basic characteristics of the PSF detector in comparison with the ionisation chamber.

MATERIALS AND METHODS

In this experiment, a self-produced PSF detector with a long detection length of 50 cm was used. The authors also used CTDI-standard PMMA head and body phantoms of 15 cm in length and 16 or 32 cm in diameter. An examination of position dependence was performed using diagnostic X-ray equipment UD 150L-30 (SHIMADZU Co. Ltd., Kyoto, Japan), whereas examinations of dependencies for energy, dose rate and slice thickness were performed using X-ray CT system (Alexion TSX-033A, TOSHIBA Co. Ltd., Tokyo, Japan).

The PSF detector

The authors used a PSF SCSF-81 (Kuraray Co. Ltd., Tokyo, Japan) as an X-ray detector. PSF is a light fibre made of scintillating plastic, the atomic number of which is effectively the same as that in human tissue. This makes it convenient to measure the absorbed dose. PSF has a double-layered structure. The core of the PSF is polystyrene resin, whereas the cladding is polymethyl methacrylate (PMMA) resin. The density of the SCSF-81 is 1.05 g cm^{-3}, which is almost equivalent to water, the diameter is very narrow (1 cm), the decay time is very short (2.4 ns) and the attenuation length (the length at which the light intensity is 1 e^{-1} from the point of light emission) is rather long (3.5 m)[10].

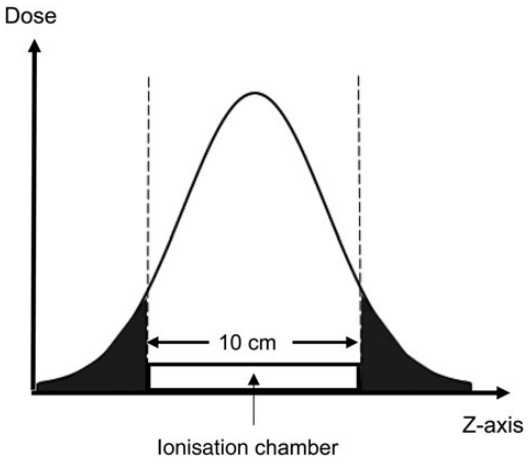

Figure 1. The dose distribution in a single CT scan. Shaded portion in this figure is produced due to X-ray absorption and scattering in the phantom.

The construction of the PSF detector used in this study is shown in Figure 2. The PSF emits lights at a point in response to X-ray irradiation, which is transmitted to a multi-pixel photon counter (MPPC). The MPPC is a photodetector that converts lights to electrical signals. It replaces the conventional photomultiplier tube (PMT). The output pulses counted by the MPPC are recorded and stored in a computer via an USB connection.

The MPPC module, C10507-11-050C (Hamamatsu photonics K.K., Hamamatsu, Japan), was used as an X-ray photon counting detector[11]. The MPPC, S10262-11-050C (Hamamatsu photonics K.K.) has an effective photosensitive area of 1 mm^2, a pixel number of 400 and a pixel size of 50 μm. The MPPC has peak quantum efficiency at a wavelength of 440 nm. In this study, the pulse-counting mode was selected in which the number of output pulses was digitally counted only when the pulses exceeded a pre-determined threshold. In the MPPC, output pulses are produced not only by photons but also by thermal excitation noise (dark count) since the MPPC is a solid-state device. The dark count of the MPPC is output as the level of a 1 p.e. pulse, which makes it difficult to distinguish the thermal excitation noise from a real 1 p.e. event[12]. Therefore, setting the optimum threshold is important. Data acquisition was carried out by a computer using the provided sample software.

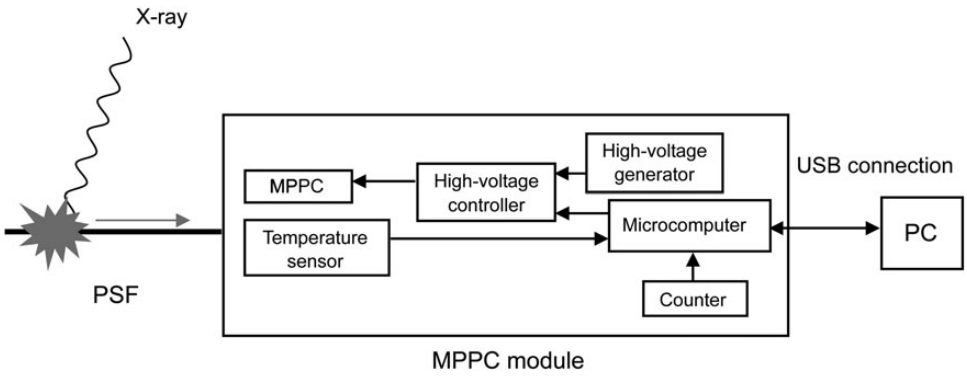

Figure 2. The construction of the PSF detector.

Threshold setting in MPPC

In dosimetry it is necessary to select the optimum threshold (the photon equivalent, p.e.), according to the number of incident photons in the MPPC. A 1 p.e. pulse is equivalent to the pulse obtained when one photon is detected. The threshold can be set within the range of 0.5–7.5 p.e. in this MPPC sample application. When the threshold is set to 0.5 p.e., the number of detected photons can be determined by measuring the number of pulses exceeding the threshold. Therefore, an experiment was performed to determine the optimum threshold for the amount of incident photons using diagnostic X-ray equipment, and the linearity between the tube current and detector output was examined. In addition, setting the threshold of 0.5 p.e. may lead to high dark count, and so the authors removed the dark count from the counting results. The conditions of the X-ray exposure were fixed at 80 kV, 0.1 s, 1 × 1 cm in irradiation field, X-ray tube focus-to-detector distance of 100 cm and irradiation position of 5 cm (distance from the connection between the PSF and the MPPC). On the other hand, tube currents and thresholds were 100, 160, 200, 250 and 300 mA, and 0.5–5.5 p.e. (in increments of 1.0 p.e.), respectively.

Position dependence

The geometry of measurement is shown in Figure 3. A 2-mm-thick lead plate with a slit of 1 × 2 cm was set between the X-ray tube and the PSF detector in order to make a narrow beam and ensure the appropriate irradiation of the fibre. The irradiation position was moved in 5-cm increments from a position of 10 cm from the connection between the PSF and the MPPC to 45 cm, and the output was measured at each position to examine the uniformity of sensitivity in response to the differences of measurement position. Exposure conditions were 80 or 120 kV, 200 mA and 0.1 s. The lead plate was placed at 70 cm from the X-ray tube. The fibre was irradiated in parallel to the floor, to avoid the scattered X-rays from the floor.

Figure 3. The geometry for measuring position dependence.

Energy dependence

The authors examined the energy dependence of the detector sensitivity by applying the following tube voltage settings: 80, 100, 120 and 135 kV. First, the PSF was fixed in the central hole at the midpoint of the 16-cm phantom using a self-made acrylic bar with an inner hole. Then, the midpoint of the PSF was aligned with the midpoint of the phantom and the rotation centre of the CT gantry. The midpoint of the fibre (25 cm) was then irradiated. The scanning conditions were 80–135 kV, 50 mA, 0.75 s/rot and slice thickness of 2 mm for energy dependence experiment. The tube voltage for the experiments of dose rate dependence and slice thickness dependence was 120 kV.

Dose rate dependence

The arrangement of the PSF detector and the phantom is shown in Figure 4. The exposure dose was measured in air and in the central holes of the 16- and 32-cm CTDI phantoms using an ionisation chamber, with the phantoms fixed on the couch. The outputs were measured by the PSF detector in the same way and compared with the results obtained by the ionisation chamber. The authors investigated the linearity between the dose rate and count rate by changing the tube current: 10, 30, 50, 100, 150, 200, 250 and 300 mA.

Slice thickness dependence

The authors compared the PSF detector and ionisation chamber outputs by changing the slice thickness (1, 2, 3 and 4 mm) in order to verify whether a slope of the response of the PSF detector is the same as that of ionisation chamber. The arrangement of the PSF detector and the phantom was the same as that shown in the dose rate dependence experiment.

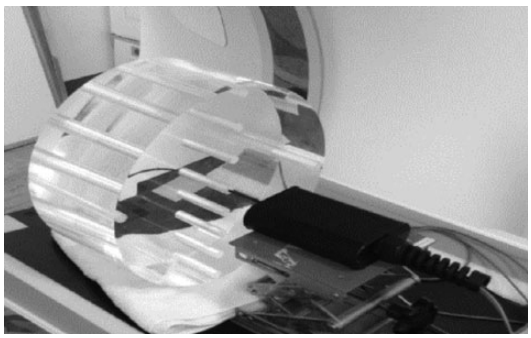

Figure 4. The arrangement of the PSF detector and the phantom for measuring dose rate dependence and slice thickness dependence.

RESULTS

Threshold setting in MPPC

As shown in Figure 5, the degree of linearity between the tube current and detector output was adequate at each threshold, and, in this study, the authors adopted a threshold of 0.5 p.e. at which the coefficient of determination was the highest ($R^2 = 0.993$).

Position dependence

As shown in Figure 6, output from the PSF detector decreased exponentially as the distance from the connection increased because the lights transmitted in the fibre decayed following an exponential function. The differences between the maximum output at 10 cm from the connection and the minimum output at 45 cm were ~18.5 and 22.9 % at 120 and 80 kV, respectively. The attenuation curve in the figure was approximated using one exponential function. The effective attenuation length based on the fitted curve was 3.04 and 2.57 m at 120 and 80 kV, respectively, and these values were shorter than the nominal length of 3.5 m. This finding might be due to small imperfections, such as scratches, which would prevent light propagation[13].

Energy dependence

In Figure 7, the X-ray effective energies of the horizontal axis were calculated in reference to the values of a previously published study[14]. The ratios of the PSF detector outputs to air kerma, which were converted from the exposure dose (detector sensitivity), were plotted on the left vertical axis. The right vertical axis shows the mass energy absorption coefficient[15] ratios of polystyrene (the material in the PSF) to air. These values were normalised by the values at a voltage of 135 kV. The sensitivity of the detector increased as X-ray effective energy increased and changed ~20 % from 80 to 135 kV. At each energy, the ratio of the detector output to air kerma was in agreement with that of the mass energy absorption coefficient between polystyrene and air, within an error of 3 %.

Dose rate dependence

Figure 8 shows the relationship between the tube current and dose rate or count rate. Figure 9 shows

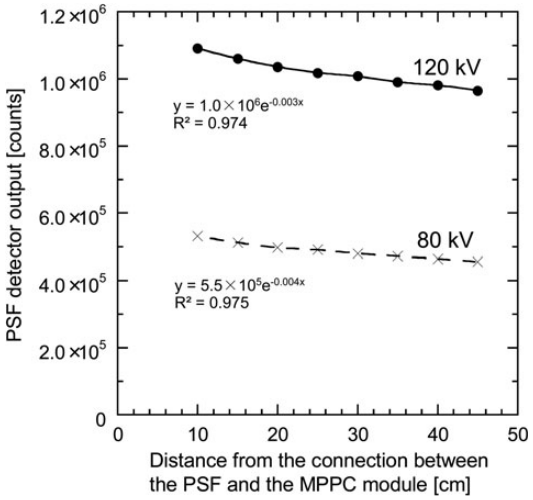

Figure 6. Position dependence at two different tube voltages of 120 and 80 kV.

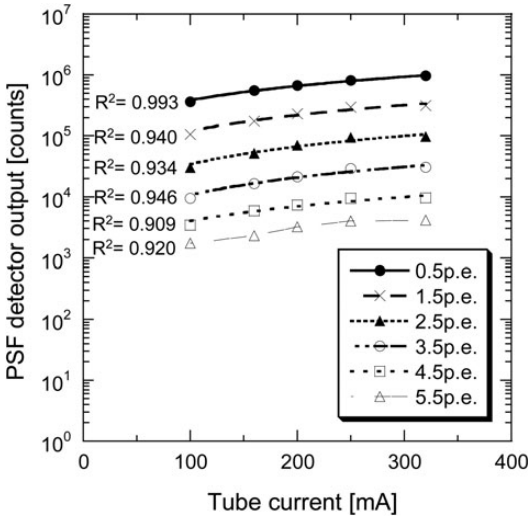

Figure 5. The relationship between the tube current and the PSF detector output by changing the threshold.

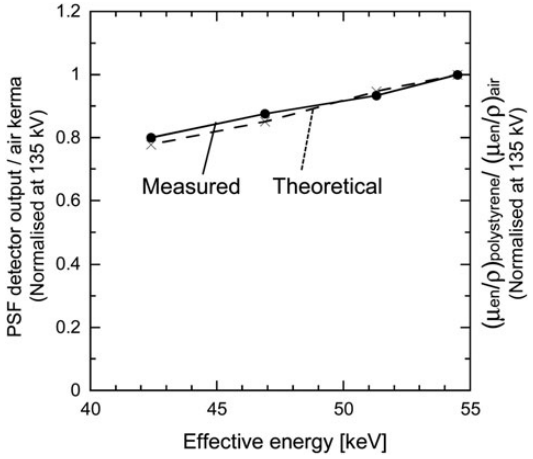

Figure 7. Comparison of energy dependence of measured values and theoretical values.

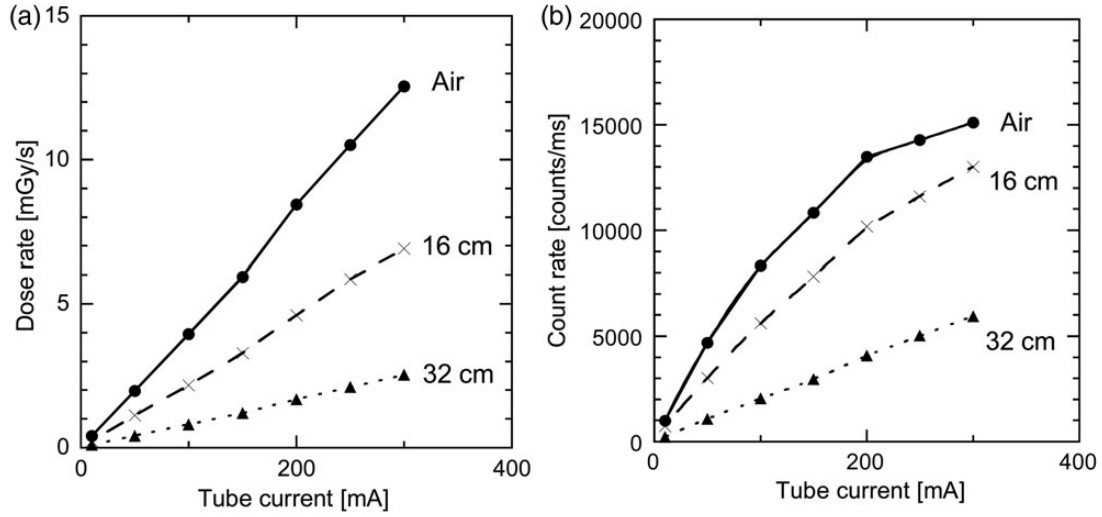

Figure 8. (**a**) The relationship between the tube current and dose rate. (**b**) The relationship between the tube current and count rate.

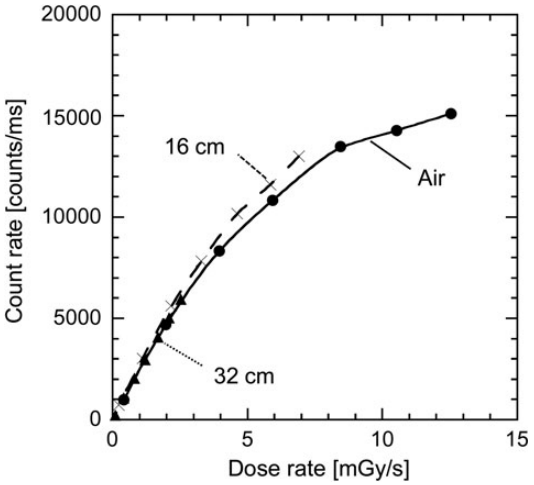

Figure 9. The relationship between the dose rate and count rate.

the relationship between the dose rate and count rate. As the figure demonstrates, excellent linearity between the tube current and dose rate was observed when using the ionisation chamber. On the other hand, the linearity of the PSF detector was good in the 32-cm phantom, although it decreased at a count rate of 10 000 counts ms^{-1} and dose rate of 5 mGy s^{-1} in air and in the 16-cm phantom.

Slice thickness dependence

In Figure 10, the slice thickness was plotted on the horizontal axis, and air kerma and the detector output were plotted on the vertical axis. The relationship between the slice thickness and the PSF detector output was non-linear in air, as shown in Figure 10b. The doses obtained by the PSF detector exceeded those obtained by the ionisation chamber when the detector output was calibrated by the value at a slice thickness of 1 mm in air using the ionisation chamber.

DISCUSSION

In this study, the authors assessed the basic characteristics of CTDI measurements using a PSF detector, which has a longer detection length than a generally used ionisation chamber.

Position dependence

The output from the PSF detector varied about $\pm 20\,\%$ with changes in the irradiation position. This was due to light attenuation in the fibre. Therefore, correcting the sensitivity along the axis of the fibre is necessary to minimise errors; however, the variation of the output is not an important matter if the midpoint of the fibre is irradiated at each measurement. Koyama *et al.* suggested that uniform sensitivity could be obtained, even if the irradiation positions were changed, by installing two PMTs (both ends of the fibre) and then processing the signals[7].

Energy dependence

The sensitivity of the detector depended on X-ray energy and increased as X-ray energy increased. Figure 7 indicated that the ratios of the PSF detector

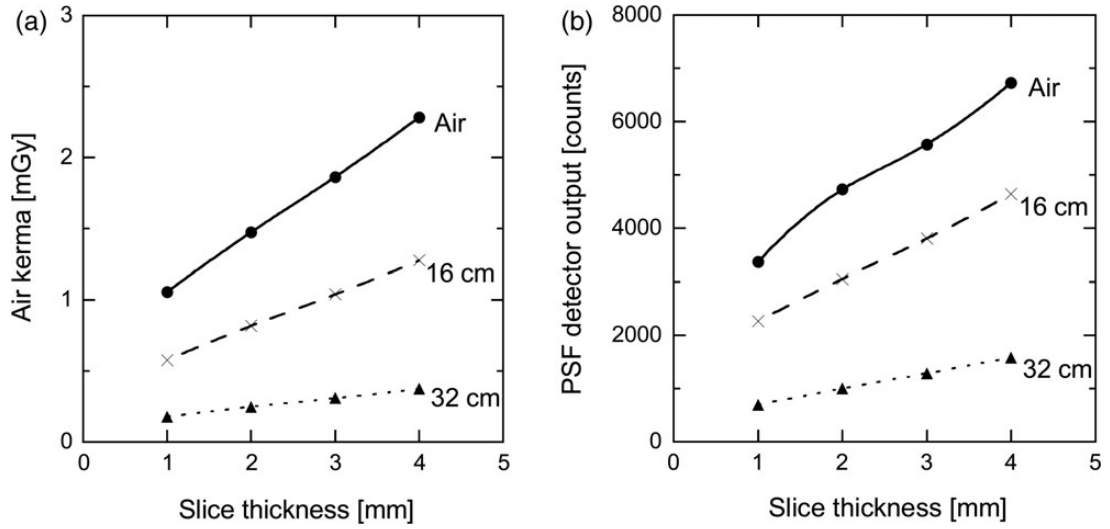

Figure 10. (**a**) The relationship between the slice thickness and air kerma. (**b**) The relationship between the slice thickness and the PSF detector output.

outputs to air kerma were almost consistent with the theoretical values of the mass energy absorption coefficient ratios of polystyrene and air. One of the reasons why these ratios were not completely consistent is that the X-ray energy spectrum of CT is continuous spectrum whereas the average X-ray effective energies were treated discretely in the calculation. As the tube voltage was normalised at 135 kV, the detector sensitivity varied approximately 20 % from 80 to 135 kV (effective energy: from 42.4 to 54.5 keV). As shown in Figure 7, if the relationship between the effective energy and detector sensitivity on each type of equipment is known, the correction for energy dependence is possible.

Dose rate dependence

A good linearity was observed between the tube current and dose rate using the ionisation chamber. For the PSF detector, however, the outputs piled up at a high count rate, which resulted in count loss. One of the reasons for the pile-up was that the photon detection efficiency of the detector was high. This is mainly due to matching of the emission peak in the wavelength (437 nm) of the PSF SCSF-81 and the peak quantum efficiency in the wavelength (440 nm) of the MPPC used in this study. Decreasing the detection efficiency of the detector is necessary to avoid the pile-up. To accomplish this, it would be necessary to decrease the amount of luminescence from the PSF by changing to another PSF with a different wavelength or to extend the dynamic range of the MPPC to facilitate the rapid measurement of the emitted light. Moreover, the threshold setting in the MPPC module had strong influence on the pile-up. As mentioned earlier, the dark count was contained in the output pulses. It would be possible to reduce the dark count by raising the threshold. This would lower the quantity of the pulses that was output from the MPPC. However, if the threshold is raised too high, it is possible that the original photons would not be counted. Thus, the determination of the exact threshold is important. Besides, shortening the length of the PSF and reducing the diameter may be effective methods to correct for the pile-up. The optimum length of the PSF needs to be determined in the future work.

Slice thickness dependence

In the slice thickness experiments, the values measured by the ionisation chamber and the PSF detector showed almost the same tendency to increase. There was non-linearity in the measurement in air using the PSF detector due to measurement errors. Two factors that may have been involved in the error were an increase in the temperature of the detector and a change in detector sensitivity during the experiment. Further investigation may elucidate the cause of the error.

One limitation associated with this study is that the authors assessed the doses with the pulse-counting mode, as mentioned earlier, and, in this mode, energy information cannot be obtained. Attix[16] stated that 'It should be apparent that for dosimetry of gamma-rays or electrons, either the PM-tube output should be measured as an electric current or the pulse-heights must be analyzed and calibrated in terms of dose.' The authors were aware of this issue; however, they considered that it would be possible to perform dosimetry with a pulse-counting mode PSF detector. The

presence of energy dependence does not matter in dosimetry under the condition of fixed energy. Therefore, the doses are derived from the PSF detector output by calibrating the device with a reference dosemeter for each condition and type of equipment.

CONCLUSION

In this study, the basic characteristics of the PSF detector were evaluated. Except for the situations in which a high dose rate was encountered, the PSF detector may be able to evaluate radiation doses within an uncertainty of 20 % using a reference dosemeter. This detector may be useful for CT, low-dose-rate dosimetry with calibration under the condition of fixed energy.

FUNDING

This work was supported by JSPS KAKENHI Grant Number 25750164.

REFERENCES

1. OECD. *OECD Health Statistics 2015* (2015). Available on http://data.oecd.org/healtheqt/computed-tomography-ct-scanners.htm (3 September 2015, date last accessed).
2. Bauhs, J. A., Vrieze, T. J., Primak, A. N., Bruesewitz, M. R. and McCollough, C. H. *CT dosimetry: comparison of measurement techniques and devices.* RadioGraphics. **28**, 245–253 (2008).
3. International Commission on Radiological Protection Publication 87. *Managing patient dose in computed tomography.* Annals of the ICRP (2000).
4. Shope, T. B., Gagne, R. M. and Johnson, G. C. *A method for describing the doses delivered by transmission x-ray computed tomography.* Med. Phys. **8**, 488–495 (1981).
5. AAPM Report No.111. *Comprehensive methodology for the evaluation of radiation dose in x-ray computed tomography.* Report of AAPM Task Group 111: The Future of CT Dosimetry. (2010).
6. International Commission on Radiation Units and Measurements Report No.87. *Radiation dose and image-quality assessment in computed tomography* (2012).
7. Koyama, S., Aoyama, T. and Maekoshi, H. *Development of a scintillating fiber dosimetry for X-ray CT devices.* Jpn. J. Radiol. Technol. **55**, 1027–1035 (1999).
8. McCollough, C. H., Zink, F. E. and Morin, R. L. *Radiation dosimetry for electron beam CT.* Radiology. **192**, 637–643 (1994).
9. Beddar, A. S., Mackie, T. R. and Attix, F. H. *Water-equivalent plastic scintillation detectors or high-energy beam dosimetry. I. Physical characteristics and theoretical consideration.* Phys. Med. Biol. **37**, 1883–1900 (1992).
10. Kuraray Co. Ltd. Available on http://kuraraypsf.jp/psf/index.html (3 September 2015, date last accessed).
11. Hamamatsu Photonics K.K. Available on http://www.hamamatsu.com/jp/en/product/category/3100/4004/index.html (September 2015, date last accessed).
12. Yamamoto, K., Yamamura, K., Sato, K., Ota, T., Suzuki, H. and Ohsuka, S. *Development of Multi-Pixel Photon Counter (MPPC).* IEEE Nucl. Sci. Symp. Conf. Rec. **2**, 1094–1097 (2007).
13. Amos, N. A., Bross, A. D. and Lundin, M. C. *Optical attenuation length measurements of scintillating fibers.* Nucl. Instrum. Methods. **297**, 396–403 (1990).
14. Kondo, H., Matsubara, K., Hirosawa, A. and Koshida, K. *A Comparison of several convenient methods of estimating effective energy in x-ray computed tomography [in Japanese].* Jpn. J. Radiol. Technol. **70**, 453–460 (2014).
15. Seltzer, S. M. and Hubbell, J. H. *Tables and graphs of photon mass attenuation coefficients and mass energy-absorption coefficients for photon energies 1 keV to 20 MeV for elements Z=1 to 92 and some dosimetric materials.* Jap. Soc. Radiol. Technol. (1995).
16. Attix, F. H. *Introduction to Radiological Physics and Radiation Dosimetry.* Wiley (1986).